

RESEARCH PAPER

Inhibition of matrix metalloproteinase-2 improves endothelial function and prevents hypertension in insulin-resistant rats

PR Nagareddy*, PS Rajput, H Vasudevan, B McClure, U Kumar, KM MacLeod and JH McNeill

Faculty of Pharmaceutical Sciences, The University of British Columbia, Vancouver, BC, Canada

Correspondence

Dr John H McNeill, Faculty of Pharmaceutical Sciences, 2146 East Mall, The University of British Columbia, Vancouver, BC, Canada, V6T 1Z3. E-mail: jmcneill@interchange.ubc.ca

*Current address: Department of Medicine, Columbia University, 630 W, 168th Street, New York, NY 10032, USA.

Keywords

matrix metalloproteinase; insulin resistance; hypertension; endothelial dysfunction; fructose; heat shock protein 90

Received

1 December 2010

Revised

7 June 2011

Accepted

29 Jun 2011

BACKGROUND AND PURPOSE

Insulin resistance is often found to be associated with high blood pressure. We propose that in insulin-resistant hypertension, endothelial dysfunction is the consequence of increased activity of vascular MMP-2. As MMP-2 proteolytically cleaves a number of extracellular matrix proteins, we hypothesized that MMP-2 impairs endothelial function by proteolytic degradation of endothelial NOS (eNOS) or its cofactor, heat shock protein 90 (HSP90).

EXPERIMENTAL APPROACH

We tested our hypothesis in bovine coronary artery endothelial cells and fructose-fed hypertensive rats (FHR), a model of acquired systolic hypertension and insulin resistance.

KEY RESULTS

Treatment of FHRs with the MMP inhibitor doxycycline, preserved endothelial function as well as prevented the development of hypertension, suggesting that MMPs impair endothelial function. Furthermore, incubating endothelial cells *in vitro* with a recombinant MMP-2 decreased NO production in a dose-dependent manner. Using substrate cleavage assays and immunofluorescence microscopy studies, we found that MMP-2 not only cleaves and degrades HSP90, an eNOS cofactor but also co-localizes with both eNOS and HSP90 in endothelial cells, suggesting that MMPs functionally interact with the eNOS system. Treatment of FHRs with doxycycline attenuated the decrease in eNOS and HSP90 expression but did not improve insulin sensitivity.

CONCLUSIONS AND IMPLICATIONS

Our data suggest that increased activity of MMP-2 in FHRs impairs endothelial function and promotes hypertension. Inhibition of MMP-2 could be a potential therapeutic strategy for the management of hypertension.

Abbreviations

PKB, protein kinase B; Ang II, angiotensin II; APMA, p-aminophenyl mercuric acetate; BCAE cells, bovine coronary artery endothelial cells; Con A, concanavalin A; EGFR, epidermal growth factor receptor; EGM, endothelial growth medium; FHR, fructose hypertensive rat HSP90, heat shock protein 90; ISI, insulin sensitivity index; L-NAME, N^G-nitro-L-arginine methyl ester; PE, phenylephrine; SMA, superior mesenteric artery; TIMP, tissue inhibitor of MMP

Introduction

Insulin resistance is often found to be associated with high blood pressure in both humans and several animal models (Reaven, 1991). It has been reported that a vast number of hypertensive patients are also insulin-resistant (Zavaroni *et al.*, 1992). Individuals with insulin resistance often exhibit changes in the behaviour of blood vessels with characteristic abnormalities in vascular reactivity, changes in several key regulators in endothelium, and an increased risk of vascular inflammation all of which could contribute to endothelial dysfunction and the development of hypertension (Hsueh and Law, 1999; Kendall and Harmel, 2002).

Despite major research efforts, it remains uncertain what causes hypertension in insulin resistance or the metabolic syndrome. Regardless of the cause, a large body of evidence invariably demonstrates that endothelial dysfunction is a hallmark of hypertension (John and Schmieder, 2000; Panza *et al.*, 1994). Interestingly, in insulin resistance, elevated blood pressure and endothelial dysfunction are also associated with elevated plasma levels of catecholamines and other vasoconstrictor GPCR agonists such as angiotensin II (Ang II), thromboxane A₂ and endothelin I (Tran *et al.*, 2009). We have proposed that vascular MMPs, which are activated by vasoconstrictor GPCR agonists play a major role in the aetiology of insulin-resistant hypertension *via* the transactivation of the epidermal growth factor receptor (EGFR) (Nagareddy *et al.*, 2010).

In addition to the transactivation of the EGFR, MMPs have been reported to proteolytically cleave a large number of membrane proteins including the extracellular domain of the insulin receptor (DeLano and Schmid-Schonbein, 2008), vascular endothelial growth factor receptor-2 (Tran *et al.*, 2010), and more recently the cleavage of β_2 -adrenoceptors in spontaneously hypertensive rats and thereby promote hypertension (Rodrigues *et al.*, 2010). Further, several studies have demonstrated that pharmacological inhibition of MMPs reduces vasoconstriction in isolated arterial rings and reduces blood pressure in animal models of hypertension (Flamant *et al.*, 2003; Florian and Watts, 1999; Hao *et al.*, 2004). In addition to their effect on arterial constriction (Rodrigues *et al.*, 2010), MMP inhibitors can also block hypertension caused by capillary rarefaction (DeLano and Schmid-Schonbein, 2008), which is due to endothelial cell apoptosis (Tran *et al.*, 2010), suggesting that MMPs promote hypertension by different mechanisms.

We previously demonstrated increased expression of contractile proteins such as myosin light chain kinase and myosin light chain II in insulin resistant vascular smooth muscle cells. Inhibition of MMPs or the EGFR reduced the expression of contractile proteins and their transcriptional activators in insulin resistant vascular smooth muscle cells (Nagareddy *et al.*, 2010). Taken together, these results suggest that inhibition of MMPs may provide a potential strategy for treatment of hypertension in insulin resistance and/or metabolic syndrome. Endothelial dysfunction is one of the main contributors to hypertension in insulin resistance, therefore, we reasoned that MMPs might play a role in the impairment of endothelial function. In the present study, we investigated the role of MMP-2 in endothelial dysfunction and its contri-

bution to the development of hypertension in high fructose diet fed rats, a model of acquired systolic hypertension and insulin resistance. Further, using drug interventions, we sought to determine the long-term effects of MMP-2 inhibition *in vivo* on insulin resistance, endothelial function and blood pressure.

Methods

Animals

All animal care and experimental procedures complied with the Guide for the Care and Use of Laboratory Animals published by the US National Institutes of Health (NIH Publication no. 85-23, revised 1996) and were approved by Institutional Animal Care Committee. Thirty-two male Wistar rats weighing between 280 and 300 g were randomly divided into four equal groups: control (C), control treated with doxycycline, a broad spectrum MMP inhibitor (CD), fructose-fed (F), fructose-fed and treated with doxycycline (FD). Animals were allowed access to food and water *ad libitum*. Rats in control groups received normal rat chow while the rats in the fructose groups were given a diet containing high fructose (60%) for 10 weeks to render them insulin-resistant and hypertensive. Following 6 weeks of fructose feeding, the rats in CD and FD groups were administered doxycycline at a dose of 20 mg·kg⁻¹, daily (Hao *et al.*, 2004; Chung *et al.*, 2008) by oral gavage for 4 weeks until termination. Basal blood pressure (at week 6) and the final blood pressure (at week 10) were measured in conscious rats using the indirect tail cuff method as described previously (Galipeau *et al.*, 2002). At the end of the treatment period an oral glucose tolerance test (OGTT) was performed. At death, blood was collected from the rats following a 5 h fast for measuring glucose, insulin and cholesterol. Animals were killed over a period of 6 days by i.p. administration of pentobarbital (65 mg·kg⁻¹, body weight) and the superior mesenteric artery (SMA) was isolated, removed and cleaned of excess adipose and connective tissues. Some of the SMA tissues were used immediately for vascular reactivity studies and for determination of MMP-2 activity using zymography, after which they were snap frozen in liquid nitrogen and stored at -70°C for Western blot studies.

OGTT and insulin sensitivity index (ISI)

At the end of treatment an OGTT was performed by administration of glucose at a dose of 1 g·kg⁻¹ to overnight fasted rats. Blood samples from the tail vein were taken before, and 10, 20, 30 and 60 min after administration of the glucose load. Plasma was separated by centrifugation and stored at -70°C until assayed for glucose and insulin. Insulin sensitivity following the OGTT was estimated using the formula of Matsuda and DeFronzo (Matsuda and DeFronzo, 1999) where $ISI = 100/\text{square root}[(\text{mean plasma glucose} \times \text{mean plasma insulin}) \times (\text{fasting plasma glucose} \times \text{fasting plasma insulin})]$.

Biochemical measurements

Plasma glucose was measured using an enzymatic colorimetric assay kit (Roche Diagnostics) and a Beckman Glucose

Analyzer. Plasma insulin was determined using a double antibody RIA kit from Linco Research Diagnostics, St. Charles, MO, USA.

Ex vivo vascular reactivity studies

Tissue rings of length 3–4 mm with intact endothelium were dissected from the SMA and appended onto glass hooks, which were then mounted in a 20 mL isolated tissue bath containing carboxygenated (95% O₂-5% CO₂) Krebs-Ringer buffer at 37°C. Tissues were primed twice with 40 mM KCl followed by assessment of endothelial integrity using ACh. Later, the tissues were assessed for changes in contraction to phenylephrine (PE) (10⁻⁹ to 10⁻⁴ M), after which they were precontracted with the ED₇₀ dose of PE, and relaxation responses to increasing concentrations of ACh (10⁻⁹ to 10⁻⁴ M) were obtained. Alterations in responses to ACh were compared between control and fructose-fed animals treated with or without doxycycline. The tissues were washed and incubated with a non-selective NOS inhibitor, N^G-nitro-L-arginine methyl ester (L-NAME, 10⁻⁶ M) for 20 min, and responses to ACh in pre-contracted tissues were obtained as described above. Responses to PE are reported as mg·mm⁻² in the SMA and as a percentage of maximum KCl contraction. Responses to ACh are reported as % relaxation in tissue pre-contracted by a ED₇₀ dose of PE.

Cell culture studies

Bovine coronary arterial endothelial cells (BCAE cells, Clonetics) were cultured in endothelial growth medium (EGM) supplemented with EGM-MV Bullet Kit (Lonza) at 37°C in a 5% CO₂ humidified incubator. Passages 4–6 were used for all experiments. BCAE cells were plated in six-well plates and grown until they reach ~70% confluence. All cells were deprived of serum overnight by placing them in media without growth factors before the treatment with inhibitor/agonists.

NO measurements

Cells were washed with PBS and pre-incubated with or without 1 mM L-NAME and 1 to 8 pM of human recombinant MMP-2 (activated with p-aminophenyl mercuric acetate, 1 mM APMA) or its vehicle for 2 h. The medium was removed and the cells in the presence of L-arginine (25 µM) were incubated with or without L-NAME and calcium ionophore, A-23187 (5 µM) for 30 min at 37°C. The cells were immediately lysed with cell lysis reagent and NO levels in the lysate were measured using a commercially available fluorimetric kit (Cayman Chemical Company, MI).

Co-localization studies

BCAE cells plated on poly-D-lysine coated cover slips were allowed to grow up to 70% confluency. On the day of the experiment, cells were stimulated with calcium ionophore (A-23187) for 30 min. To activate MMP-2, some cells were incubated with concanavalin A (Con A, 20 µg·mL⁻¹) for 24 h before stimulating with A-23187. Cells were fixed with 4% paraformaldehyde, washed with PBS and blocked using 5% normal goat serum for 1 h at room temperature. This was followed by incubation with a combination of rabbit polyclonal MMP-2 with either mouse monoclonal endothelial

NOS (eNOS) or mouse monoclonal heat shock protein 90 (HSP90) primary antibodies overnight at 4°C. Subsequently the cells were washed with PBS and incubated with goat anti-mouse Alexa-488 (green) and goat anti-rabbit Alexa-594 (red) secondary antibodies for 1 h at room temperature. Cells were washed with PBS and cover slips mounted and observed using a Leica DMLB microscope attached with the Retiga 2000R camera. The extent of co-localization was determined using ImageJ software (National Institute of Health) and a co-localization highlighter plug-in (P. Bourdoncle, Institute Jacques Monod, Service Imagerie, Paris, France). This plug-in generates an image of co-localized pixels by merging the red and green 8-bit channels and highlights the co-localized pixels in white (Display value = 255). For each treatment condition, the threshold for both the channels was set to 50 and intensity ratio to 50% for consistency of the data.

Substrate cleavage assay

Substrate cleavage assay was performed by incubating HSP90 with active MMP-2. Briefly, active MMP-2 was incubated with the purified human recombinant HSP90 (Enzo Life Sciences, PA) in 50 mM Tris-HCl, 200 mM NaCl, 5 mM CaCl₂ and 0.025% NaN₃ for 16 h at 37°C. Reaction products were analysed by Tris-glycine SDS-PAGE and silver-stained.

MMP-2 activity and expression

MMP-2 activity in SMA tissue releasates was measured using gelatin zymography. The releasates were subjected to SDS-PAGE (under non-reducing conditions) using 2% gelatin gels. Following electrophoresis, the gels were washed with Triton X-100 (2.5% for 3 × 20 min) and incubated at 37°C overnight in zymogram development buffer containing 50 mM Tris-HCl, pH 7.5, 200 mM NaCl, 5 mM CaCl₂, 0.02% Brij-35Tris. The gels were then stained with coomassie blue and MMPs were detected as transparent bands against the background of coomassie blue-stained undigested gelatin. The ratio of pro-MMP-2 to active-MMP-2 was used to measure MMP-2 activity. MMP-2 expression was measured by Western blotting as described previously (Nagareddy *et al.*, 2010).

Statistical analysis

Values are expressed as mean ± SEM; *n* indicates the number of rats in each group. Statistical analyses were performed using one-way ANOVA or repeated measures ANOVA (general linear models ANOVA), followed by a Newman-Keuls test, with Graphpad Prism Software and NCSS 2000 statistical software respectively. All data, except the data from vascular reactivity experiments were examined using ANOVA. The level of significance was set at *P* < 0.05.

Results

Doxycycline reduces MMP-2 activity in the arteries of fructose hypertensive rats (FHR)

Fructose feeding significantly increased MMP-2 activity and its expression in SMAs of FHRs compared with control rat

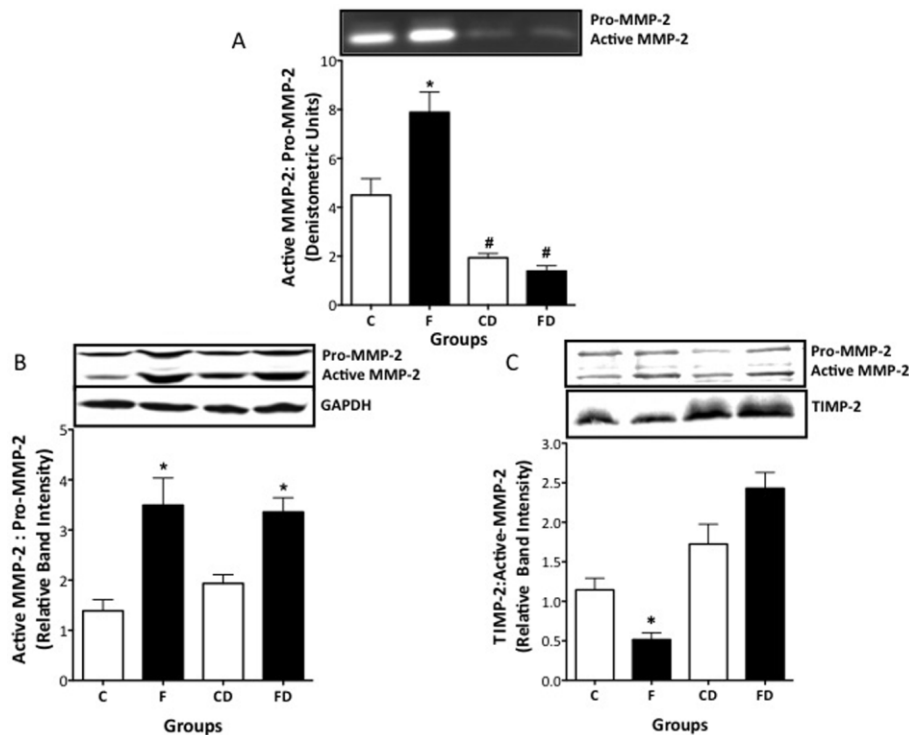


Figure 1

Effect of doxycycline (D) on the activity and expression of MMP-2 and TIMP-2 in the SMAs of control and FHRs. (A) Representative zymogram and quantitative analysis of MMP-2 activity as measured by the ratio of active MMP-2 to pro-MMP-2 in the SMA. For zymography experiments, small pieces of SMAs of equal weight from control and FHRs (treated with doxycycline for 4 weeks) were incubated in Krebs-Ringer buffer and the basal MMP-2 activity in the releasate was determined by gelatin zymography. (B) Representative Western blot showing MMP-2 expression in the SMAs, with GAPDH as a loading control. The densitometric value of active MMP-2 was normalized to its pro-form and the relative band intensities are expressed as mean \pm SEM ($n = 8$). (C) Representative Western blot showing the expression of TIMP-2 in relation to expression of active MMP-2. The densitometric values of TIMP-2 were normalized to their corresponding active-MMP-2 densitometric values and the relative band intensities are expressed as mean \pm SEM ($n = 8$). *Different from all other groups ($P < 0.05$), #Different from C and F groups. C: control groups; F: fructose-fed rats.

arteries (Figure 1A and B). Treatment with doxycycline for 4 weeks significantly reduced MMP-2 activity both in control and FHRs but did not change the corresponding protein expression. However, doxycycline treatment significantly increased the expression of the endogenous MMP-2 inhibitor, TIMP-2 (Figure 1C). Further, the ratio of TIMP-2/MMP-2 was also increased in FD rats, suggesting that doxycycline inhibits MMP activity by increasing TIMP levels (Chung *et al.*, 2008).

Doxycycline improves endothelial function and prevents the development of hypertension in FHR

Cumulative concentration-responses curves to PE and ACh in SMAs with intact endothelium were obtained from control and fructose-fed rats (Figure 2). As previously reported (Vasudevan *et al.*, 2006), fructose feeding did not change the response to PE in these arteries (Figure 2A) but induced impaired endothelial function as demonstrated by attenuated vasorelaxant responses to ACh. Treatment with doxycycline significantly improved vascular responses to ACh in FD rats

compared with untreated fructose-fed rats (Figure 2B). Inhibition of NO production by L-NAME prevented ACh-induced vasorelaxation in SMA from all groups suggesting that decreased eNOS activity is mainly responsible for the impaired endothelial function in FHRs. Further, in fructose rats, doxycycline prevented the increase in systolic blood pressure without affecting blood pressure in control rats (Figure 2D), most likely due to an improvement in endothelial function.

To investigate whether doxycycline improved endothelial function by preserving eNOS expression and activity, we measured the levels of phospho-eNOS and total eNOS expression in SMAs from control and fructose-fed rats. Fructose feeding significantly decreased phospho-eNOS (ser1177) and total eNOS expression in SMAs compared with control rats (Figure 2E). The decrease in phospho-eNOS expression was most likely due to decreased total eNOS protein. Treatment of doxycycline preserved the phosphorylation status of eNOS as determined by the increased ratio of phospho-eNOS to total eNOS. These data suggest that MMPs might be involved in the impairment of endothelial function by acting directly on the eNOS-NO system in fructose-fed rats.

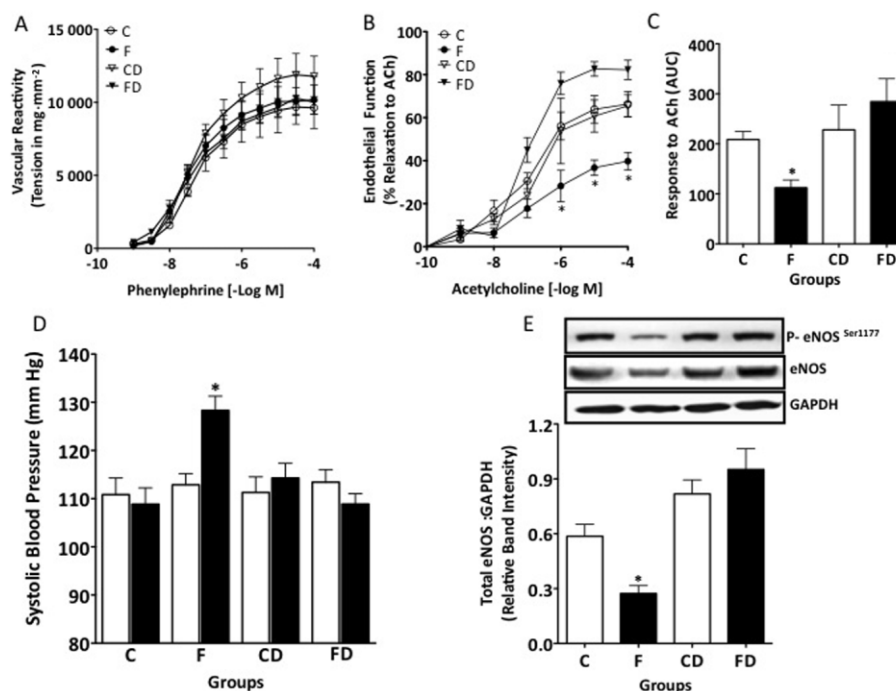


Figure 2

Effect of doxycycline treatment (D) on vascular reactivity, endothelial function, systolic blood pressure and eNOS expression in SMAs from control and FHRs. (A) Concentration response curves to increasing concentrations of PE (10^{-9} to 10^{-4} M) in SMA. (B) Concentration response curves to increasing concentration of ACh, ACh (10^{-9} to 10^{-4} M) in SMA constricted with a concentration that is ED_{70} of PE. All values are expressed as mean \pm SEM ($n = 8$). *Different from all groups ($P < 0.05$). (C) Represents area under curve (AUC) values for ACh responses. *Different from all groups ($P < 0.05$). C: control groups; F: fructose-fed rats. (D) Effect of doxycycline on systolic blood pressure in control and FHRs. Control and fructose-fed rats were treated orally with doxycycline ($20 \text{ mg} \cdot \text{kg}^{-1} \cdot \text{day}^{-1}$) for 4 weeks starting at week 6 (basal, open columns) until week 10 (final, solid columns). All values are expressed as mean \pm SEM ($n = 8$). *Different from all groups ($P < 0.05$). (E) Effect of doxycycline on eNOS expression in SMAs of control and FHRs. Representative Western blot showing phospho and total eNOS expression, with GAPDH as a loading control. The densitometric values of eNOS were normalized to their corresponding GAPDH densitometric values and the relative band intensities are expressed as mean \pm SEM ($n = 8$). *Different from all groups ($P < 0.05$). C: control groups; F: fructose-fed rats.

Inhibition of MMPs by doxycycline did not improve insulin sensitivity in FHR

The effect of MMP inhibition on insulin resistance was determined by an OGTT. Changes in glucose and insulin levels subsequent to glucose challenge are summarized in Figure 3. Fructose feeding resulted in insulin resistance as demonstrated by increased insulin secretion to glucose challenge compared with control rats (Figure 3B). Further, analysis of ISI values calculated from the OGTT revealed a significant attenuation in insulin sensitivity in fructose-fed rats (Figure 3C). Treatment with doxycycline did not improve insulin sensitivity in our model. To confirm the *in vivo* findings of OGTT, we measured the basal phosphorylation status of insulin receptor substrate 1 (IRS1) and its downstream target, protein kinase B (PKB) in aortic tissues. We found that phosphorylation of IRS1 (tyr989) and PKB (Akt; ser473) was significantly blunted in fructose group (F) compared with C, CD and FD groups. Treatment with doxycycline did not change either the expression of phospho or total IRS1/PKB level (Figure S1). These data suggest that improvement of hypertension by doxycycline in fructose-fed rats is independent of insulin resistance.

MMP-2 decreases agonist-induced NO production from endothelial cells

To further explore the cellular mechanisms underlying the MMP-2-mediated endothelial dysfunction, the interaction between MMP-2 and the eNOS-NO system was examined *in vitro* using BCAE cells. The effect of MMP-2 on agonist-stimulated NO release in BCAE cells is summarized in Figure 4. Stimulation of BCAE cells with the calcium ionophore A-23187, which promotes dissociation of eNOS from caveolin resulted in >2.5 -fold increase in total nitrite and nitrate levels compared with control cells (from $0.75 \pm 0.09 \mu\text{M}$ to $2.3 \pm 0.4 \mu\text{M}$). To understand whether the source of NO production was eNOS, the ability of A-23187 to increase NO production was determined in the presence of eNOS inhibitor, L-NAME. Treatment with L-NAME alone did not change NO levels compared with control cells (Figure 4A). However, pretreatment with L-NAME significantly reduced A-23187-stimulated NO release suggesting that NO release was due to activation of eNOS. We next determined the effect of MMP-2 on eNOS-derived NO production in response to A-23187. As shown in Figure 4B, active MMP-2 (1 to 8 pM, treated with APMA) significantly decreased NO release in response to agonist

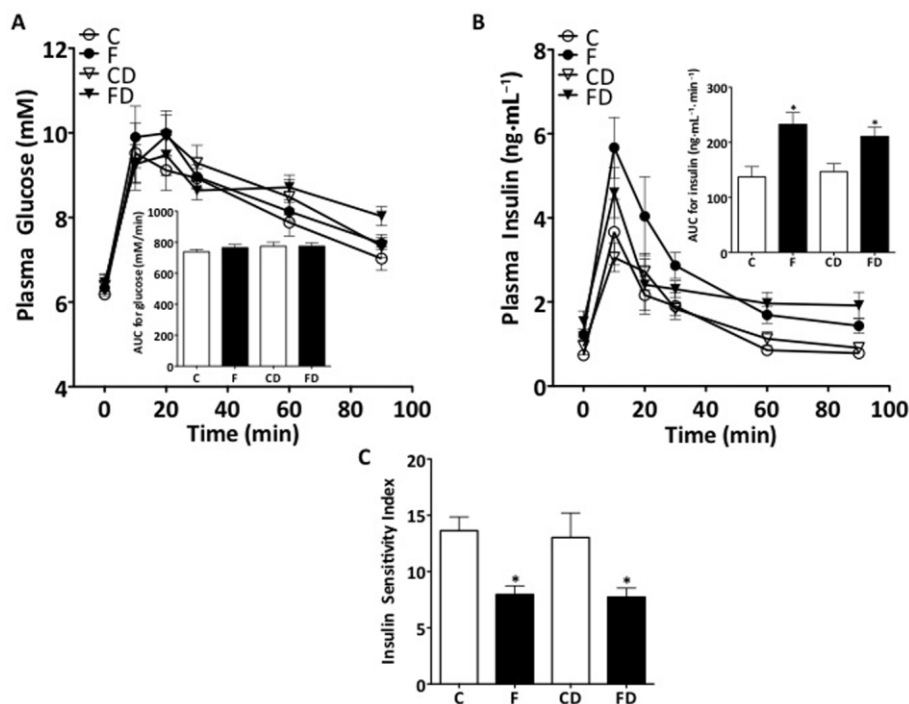


Figure 3

Effect of doxycycline treatment (D) on plasma glucose and insulin profiles following an OGTT in control and fructose-fed rats. (A) Plasma glucose (mM) and (B) plasma insulin (ng·mL⁻¹) levels before, and 10, 20, 30, 60 and 90 min after an oral glucose load of 1 g kg⁻¹ to rats fasted overnight. Figures (insets) represent area under curve (AUC) for glucose and insulin levels in control and fructose rats treated with or without doxycycline. (C) Insulin sensitivity index (ISI) values were estimated according to formula of Matsuda and DeFronzo, where $ISI = 100/\text{square root}[(\text{mean plasma glucose} \times \text{mean plasma insulin}) \times (\text{fasting plasma glucose} \times \text{fasting plasma insulin})]$. All values are expressed as mean \pm SEM ($n = 8$). *Significantly different from the control groups ($P < 0.05$). C: control groups; F: fructose-fed rats.

stimulation in a concentration-dependent manner. On the other hand, inactive MMP-2 (not treated with APMA) failed to inhibit A-23187-stimulated NO release.

MMP-2 cleaves HSP90, a cofactor for eNOS activity

To investigate if MMP-2 interferes with eNOS activity, we performed substrate cleavage assays for one of its cofactors, HSP90. As shown in Figure 5A, MMP-2 proteolytically degraded HSP90 into a number of fragments. The concentrations of MMP-2 used were too low to be detected on the gel. However, HSP90 and its degradation products are clearly visible. To confirm if HSP90 is a substrate for MMP-2 *in vivo*, we measured HSP90 expression in SMA tissue homogenates from control and fructose-fed rats. As shown in Figure 5B, there was a significant decrease in the expression of HSP90 in untreated fructose compared with all other groups. However, treatment of FHRs with doxycycline significantly improved the expression of HSP90 possibly by preventing its degradation by MMP-2.

MMP-2 co-localizes with HSP90 and eNOS in endothelial cells

We performed immunofluorescence studies in BCAE cells, to determine if MMP-2 co-localizes with either HSP90 or eNOS.

We used Con A to stimulate MMP-2 and A-23187, a calcium ionophore to activate eNOS. As shown in Figure 6, in control cells MMP-2 immunostaining was mainly in the perinuclear zone and punctuated staining in cytoplasm (Figure 6B). Stimulation of cells with Con A caused a significant redistribution of MMP-2 with greater immunostain observed near perinuclear zone (Figure 6F). However, in cells co-stimulated with Con A and A-23187, there was a marked decrease in MMP-2 immunostain near the perinuclear zone but a significant increase in the regions of plasma membrane (Figure 6J). Similarly, HSP90, which was mainly localized near the perinuclear zone in control and Con A stimulated cells (Figure 6A and E), redistributed to plasma membrane in cells co-stimulated with Con A and A-23187 (Figure 6I).

We next studied the extent of co-localization of MMP-2 and HSP90 in control cells and those co-stimulated with Con A and A-23187. In unstimulated cells, co-localization was mainly observed near the perinuclear zone (Figure 6D). The extent of co-localization (Figure S2) increased further around the perinuclear zone and spilled over to cytoplasm in cells stimulated with Con A (Figure 6H). Interestingly, in cells treated with both Con A and A-23187, there was a marked reduction in the extent of co-localization in the perinuclear zone but an increase in the cytoplasm and regions of plasma membrane (Figure 6L). This may be due to redistribution of MMP-2 from the perinuclear zone towards the cytoplasm and plasma membrane.

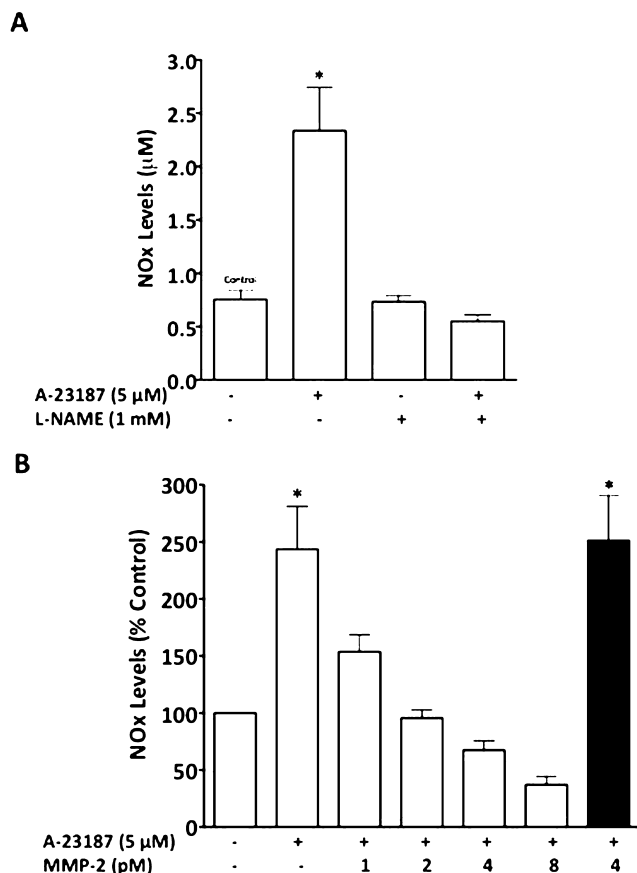


Figure 4

Effect of MMP-2 on calcium ionophore stimulated NO production in BCAE cells. (A) Total nitrite and nitrate levels (NOx) in the presence or absence of the eNOS inhibitor, L-NAME (1 mM). Results are expressed as mean \pm SEM ($n = 4$ independent experiments). *Different from all other groups ($P < 0.05$). (B) NOx levels in the presence of increasing concentrations of active MMP-2 (open columns) and inactive MMP-2 (solid column). Results are expressed as per cent control and are means \pm SEM ($n = 4$ independent experiments). *Different from control and active MMP-2 treated cells ($P < 0.05$). In all experiments, BCAE cells were pre-incubated with 1 to 8 pM of active (treated with 1 mM APMA for 2 h at 37°C or inactive human recombinant MMP-2 or its vehicle for 2 h and stimulated with the calcium ionophore, A-23187 (5 μM) for 30 min. For, L-NAME experiments, cells were incubated with L-NAME for 2 h and stimulated with ionophore.

We next examined the expression and pattern of co-localization of MMP-2 with eNOS. As shown in Figure 7, similar to HSP90, MMP-2 immunoreactivity was found mostly near the perinuclear zone in unstimulated cells. Interestingly, however, stimulation of cells with Con A alone increased the expression of both eNOS and MMP-2 immunostain in the cytoplasm and plasma membrane (Figure 7E and F). Co-stimulation with Con A and A-23187 further increased this translocation as shown by increased intensity of immunostain in the cytoplasm and plasma membrane (Figure 7I and J). Analysis of co-localization in cells co-stimulated with Con A and A-23187 (Figure S3) suggests a

decrease in the extent of overlap in the perinuclear zone perhaps due to the redistribution of MMP-2.

Discussion and conclusions

Several mechanisms have been proposed to explain the pathogenesis of hypertension associated with insulin resistance and type 2 diabetes (Kim *et al.*, 2006). We hypothesized that in insulin resistance, elevated levels of GPCR agonists such as catecholamines and other vasoactive peptides activate vascular MMPs such as MMP-2 and MMP-7, resulting in endothelial dysfunction. The important findings from the present study are: (i) hypertension in insulin resistance is associated with increased expression and activity of MMP-2; (ii) inhibition of MMP-2 activity by doxycycline prevented the development of hypertension and endothelial dysfunction; (iii) MMP-2 impaired endothelial function and eNOS activity; and (iv) HSP90 and possibly eNOS, is a substrate for proteolytic processing by MMP-2.

In the present study, using the FHR model, we studied the effect of inhibition of MMPs on vascular reactivity, endothelial function, insulin sensitivity and development of hypertension. The FHR model presents a host of metabolic abnormalities similar to that observed in the metabolic syndrome in humans (Hwang *et al.*, 1987; Johnson *et al.*, 2007). Further, many of the mechanisms linking insulin resistance to hypertension are apparent in rats fed a high fructose diet, including hyperinsulinaemia (Verma *et al.*, 1995), endothelial dysfunction (Verma *et al.*, 1996; Katakam *et al.*, 1998), increased levels of oxidative stress (Song *et al.*, 2005) and increased sympathetic nervous system activity (Verma *et al.*, 1999). Further, we have previously found that chronic fructose feeding is also associated with increased levels of plasma noradrenaline (NA), Ang II, thromboxane A₂ and endothelin I (Tran *et al.*, 2009), which are all known to activate MMPs. Treatment of FHRs with doxycycline did not change either Ang II or NA levels in plasma (data not shown).

Feeding rats with a high fructose diet not only produced the classical symptoms of metabolic syndrome such as insulin resistance, hyperinsulinaemia and hypertension (Verma *et al.*, 1995; Galipeau *et al.*, 2002; Vasudevan *et al.*, 2006) but also resulted in increased expression and activity of MMP-2 in SMAs. This increase in MMP-2 expression was associated with a decreased expression of its endogenous inhibitor, TIMP-2. It should be noted that a relative paucity of TIMP-2 in relation to MMP-2 favours increased proteolytic activity (Murphy *et al.*, 1994). Treatment of fructose-fed rats with doxycycline decreased MMP activity, a property that could be attributed to doxycycline binding to zinc/calcium at the catalytic site, blocking the active site or inducing conformational changes that render the pro-enzyme susceptible to fragmentation during activation (Smith *et al.*, 1996; Golub *et al.*, 1998). Alternatively, doxycycline could inhibit MMP activity by up-regulating the levels of the TIMPs that can bind and inactivate MMPs (Yao *et al.*, 2007) a mechanism that is supported by the findings of our present study, where doxycycline increased the levels of both TIMP-2 as well as the ratio of TIMP-2/MMP-2.

Previous studies from our laboratory and elsewhere have shown that several drug interventions that improve insulin

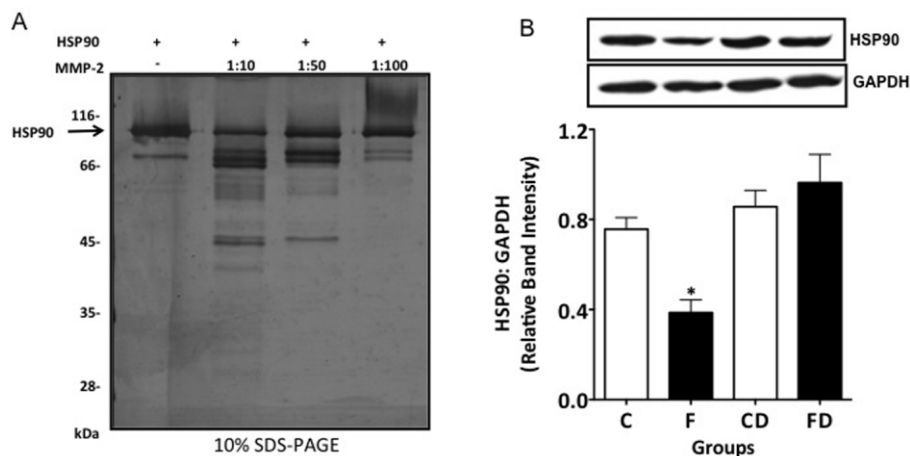


Figure 5

MMP-2 proteolytic activities on human HSP90 *in vitro* and in SMAs tissue homogenates. (A) Representative silver stained SDS-PAGE (10%) gel data from at least three replicate experiments showing degradation products of human recombinant HSP90. Increasing concentrations of HSP90 (enzyme : substrate ratio) were incubated with MMP-2 for 16 h at 37°C and the cleavage products were separated on SDS-PAGE and analysed by silver staining. The concentrations of MMPs used were too low to be detected on the gel. (B) HSP90 expression in SMAs of control and FHRs. Representative Western blot showing HSP90, with GAPDH as a loading control. The densitometric values of HSP90 were normalized to their corresponding GAPDH densitometric values and the relative band intensities are expressed as mean \pm SEM ($n = 8$). *Different from all groups ($P < 0.05$). C: control groups; F: fructose-fed rats.

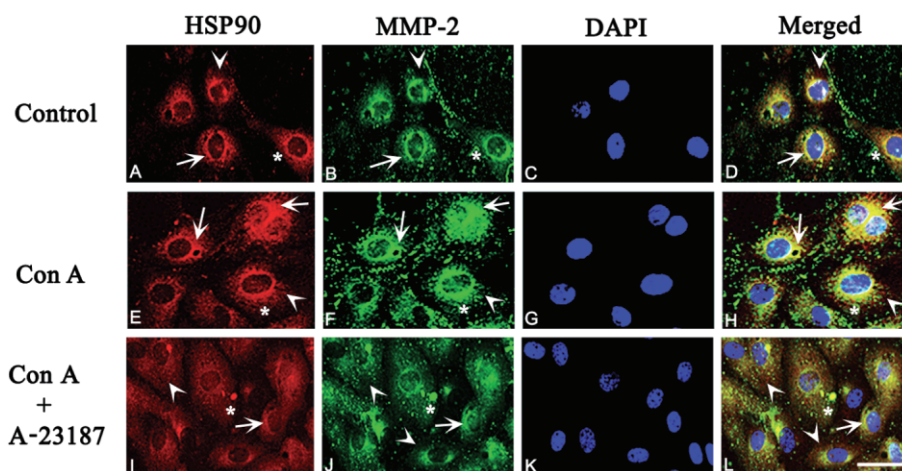


Figure 6

Representative photomicrographs illustrating the co-localization of MMP-2 and HSP90 in BCAE cells. BCAE cells were treated with MMP-2 and HSP90 antibodies for 24 h, followed by incubation with goat anti-mouse Alexa 488 (green) and goat anti-rabbit Alexa 594 (red). The co-localization of MMP-2 and HSP90 is indicated by yellow colour in the overlapped images panels D, H and L. In all the representative images arrows indicate co-localization, arrowhead represents HSP90 immunoreactivity and MMP-2 immunoreactivity is identified by an asterisk. Scale bar = 20 μ m.

sensitivity, including metformin, vanadium compounds and thiazolidinediones, can ameliorate hypertension in this model (Bhanot *et al.*, 1994; Lee *et al.*, 1994; Verma *et al.*, 1994; Kotchen *et al.*, 1997). We therefore investigated whether the improvement in hypertension in fructose-fed rats treated with doxycycline was due to changes in insulin sensitivity. Further, it has been long known that improving endothelial function improves insulin resistance and *vice*

versa (Kim *et al.*, 2006). This has led to the assumption that insulin-resistant states are associated with reduced eNOS expression, and that improving insulin sensitivity promotes NO-mediated vasodilatation by activating eNOS. Although we found reduced phosphorylation of eNOS, IRS1 and PKB (Akt) in the arteries from FHRs, improvement in endothelial function with doxycycline was not associated with changes in insulin signalling. This could be due to the differences in

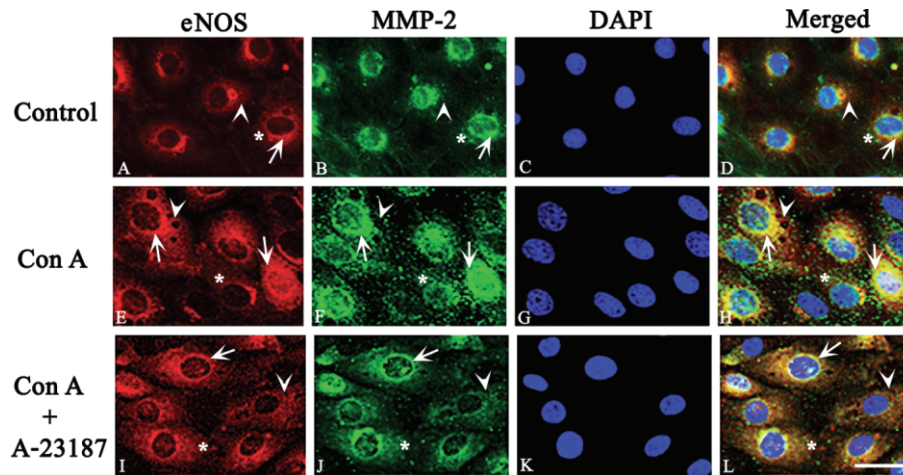


Figure 7

Representative photomicrographs illustrating co-localization of eNOS and MMP-2 in BCAA cells. eNOS positive immunoreactivity was localized by Alexa-594 (red) fluorescence and MMP-2 like immunoreactivity indicated by Alexa-488 (green). Panels A–D represent co-localization indicated by yellow colour in control cells; panels E–H represent co-localization after Con A treatment and panels I–L represent co-localization after Con A and A-23187 treatment. In all the representative panels arrows indicate co-localization, arrowhead represents eNOS immunoreactivity and MMP-2 immunoreactivity is identified by an asterisk. Scale bar = 20 μ m.

the dosage of doxycycline used, the subtype of MMP enzyme involved (MMP-2 vs. MMP-9) or, most importantly, the animal model used. Further, we did not see changes in any other metabolic parameters including plasma glucose, insulin, triglyceride or cholesterol (data not shown). Our data suggest that impaired endothelial function in FHRs was due to increased MMP activity and independent of changes in insulin sensitivity.

NO production in endothelial cells is stimulated by a variety of stimuli including mechanical forces, growth factors and peptide hormones. eNOS, which catalyzes the production of NO, is a peripheral membrane protein that is localized to endothelial plasmalemmal caveolae through an interaction with caveolin-1, a structural protein. Caveolin 1 inhibition of eNOS is relieved by calm, which causes dissociation of eNOS from caveolin. This regulatory mechanism is modified by HSP90, which binds to eNOS and facilitates displacement of caveolin by calm (Fleming and Busse, 2003). We speculated that reduced eNOS activation in insulin-resistant rats could be due to the direct interaction of MMP-2 with eNOS or HSP90 resulting in its inactivation or degradation by proteolytic cleavage (Fernandez-Patron *et al.*, 1999; 2000). In support of this argument, we found decreased expression of both eNOS (phospho and total) and HSP90 in SMAs from FHRs. Further, this was confirmed *in vitro* in endothelial cells, where incubation of active MMP-2 attenuated calcium ionophore-stimulated NO production in a dose-dependent manner.

It is unclear how exogenously added MMP-2 in our cell culture model would decrease NO production, which is presumed to take place within the caveolae, the flask-shaped invaginations of the plasma membrane. Various studies have provided evidence that MMP-2 can be localized in its proteolytically active form on the surface of cells, based on its ability to bind directly to the integrin α v β 3 receptor (Brooks

et al., 1996). One possible mechanism is that MMP-2, acting on its putative α v β 3 receptor would stimulate biochemical phosphorylation cascades involving various mediators such as Raf, Ras, MAPKs (ERKs), or Rho GTPases resulting in sub-cellular compartmentalization and traffic of MMPs into caveolae (Jiang *et al.*, 2001; Galvez *et al.*, 2004). In fact, a recent study demonstrated that MMP-2 co-localizes with caveolin-1, a major constituent of the caveolae in human endothelial cells (Puyraimond *et al.*, 2001). Alternatively, increased proteolytic activity of MMP-2 at the surface of the cell could lead to the destruction of elastic fibres or degradation of matrix resulting in the loss of eNOS activity (Chung *et al.*, 2007). Regardless of the mechanisms, our co-localization studies clearly demonstrate that MMP-2 is present within the cell cytoplasm and around the nucleus and co-localizes with both eNOS and HSP90. Our data are consistent with other studies that have demonstrated not only the intracellular localization of MMP-2 (Wang *et al.*, 2002; Kwan *et al.*, 2004; Sawicki *et al.*, 2005), but also a functional role including proteolytic processing of the eNOS/NO system components.

The results of our study suggest that vascular MMPs such as MMP-2, which is activated in conditions of insulin resistance, presumably, due to elevated levels of vasoconstrictor GPCR agonists, impair endothelial function and contribute to the development of hypertension. Considering the fact that endothelial dysfunction correlates with the development of coronary artery disease and predicts future cardiovascular events, this dysfunction needs to be considered as a central target in the treatment of hypertension, atherosclerosis or any other condition in which endothelial dysfunction is a causative factor. Taken together, these findings indicate potential therapeutic strategies to improve endothelial dysfunction and hypertension, particularly, in conditions of insulin resistance.

Acknowledgements

We thank Amanda Starr and Dr Chris Overall for their help in substrate cleavage assays. Funded by a grant to J. H. M. from the Heart and Stroke Foundation (HSFC) of BC & Yukon. P. R. N. is a recipient of Doctoral Awards from the HSFC and the Michael Smith Foundation for Health Research.

Conflict of interest

None.

References

- Bhanot S, McNeill JH, Bryer-Ash M (1994). Vanadyl sulfate prevents fructose-induced hyperinsulinemia and hypertension in rats. *Hypertension* 23: 308–312.
- Brooks PC, Stromblad S, Sanders LC, von Schalscha TL, Aimes RT, Stetler-Stevenson WG *et al.* (1996). Localization of matrix metalloproteinase MMP-2 to the surface of invasive cells by interaction with integrin alpha v beta 3. *Cell* 85: 683–693.
- Chung AW, Au Yeung K, Sandor GG, Judge DP, Dietz HC, van Breemen C (2007). Loss of elastic fiber integrity and reduction of vascular smooth muscle contraction resulting from the upregulated activities of matrix metalloproteinase-2 and -9 in the thoracic aortic aneurysm in Marfan syndrome. *Circ Res* 101: 512–522.
- Chung AW, Yang HH, Radomski MW, van Breemen C (2008). Long-term doxycycline is more effective than atenolol to prevent thoracic aortic aneurysm in marfan syndrome through the inhibition of matrix metalloproteinase-2 and -9. *Circ Res* 102: e73–e85.
- DeLano FA, Schmid-Schonbein GW (2008). Proteinase activity and receptor cleavage: mechanism for insulin resistance in the spontaneously hypertensive rat. *Hypertension* 52: 415–423.
- Fernandez-Patron C, Radomski MW, Davidge ST (1999). Vascular matrix metalloproteinase-2 cleaves big endothelin-1 yielding a novel vasoconstrictor. *Circ Res* 85: 906–911.
- Fernandez-Patron C, Stewart KG, Zhang Y, Koivunen E, Radomski MW, Davidge ST (2000). Vascular matrix metalloproteinase-2-dependent cleavage of calcitonin gene-related peptide promotes vasoconstriction. *Circ Res* 87: 670–676.
- Flamant M, Tharaux PL, Placier S, Henrion D, Coffman T, Chatziantoniou C *et al.* (2003). Epidermal growth factor receptor trans-activation mediates the tonic and fibrogenic effects of endothelin in the aortic wall of transgenic mice. *FASEB J* 17: 327–329.
- Fleming I, Busse R (2003). Molecular mechanisms involved in the regulation of the endothelial nitric oxide synthase. *Am J Physiol Regul Integr Comp Physiol* 284: R1–R12.
- Florian JA, Watts SW (1999). Epidermal growth factor: a potent vasoconstrictor in experimental hypertension. *Am J Physiol* 276 (3 Pt 2): H976–H983.
- Galipeau D, Verma S, McNeill JH (2002). Female rats are protected against fructose-induced changes in metabolism and blood pressure. *Am J Physiol Heart Circ Physiol* 283: H2478–H2484.
- Galvez BG, Matias-Roman S, Yanez-Mo M, Vicente-Manzanares M, Sanchez-Madrid F, Arroyo AG (2004). Caveolae are a novel pathway for membrane-type 1 matrix metalloproteinase traffic in human endothelial cells. *Mol Biol Cell* 15: 678–687.
- Golub LM, Lee HM, Ryan ME, Giannobile WV, Payne J, Sorsa T (1998). Tetracyclines inhibit connective tissue breakdown by multiple non-antimicrobial mechanisms. *Adv Dent Res* 12: 12–26.
- Hao L, Du M, Lopez-Campistrous A, Fernandez-Patron C (2004). Agonist-induced activation of matrix metalloproteinase-7 promotes vasoconstriction through the epidermal growth factor-receptor pathway. *Circ Res* 94: 68–76.
- Hsueh WA, Law RE (1999). Insulin signaling in the arterial wall. *Am J Cardiol* 84: 21J–24J.
- Hwang IS, Ho H, Hoffman BB, Reaven GM (1987). Fructose-induced insulin resistance and hypertension in rats. *Hypertension* 10: 512–516.
- Jiang A, Lehti K, Wang X, Weiss SJ, Keski-Oja J, Pei D (2001). Regulation of membrane-type matrix metalloproteinase 1 activity by dynamin-mediated endocytosis. *Proc Natl Acad Sci U S A* 98: 13693–13698.
- John S, Schmieder RE (2000). Impaired endothelial function in arterial hypertension and hypercholesterolemia: potential mechanisms and differences. *J Hypertens* 18: 363–374.
- Johnson RJ, Segal MS, Sautin Y, Nakagawa T, Feig DI, Kang DH *et al.* (2007). Potential role of sugar (fructose) in the epidemic of hypertension, obesity and the metabolic syndrome, diabetes, kidney disease, and cardiovascular disease. *Am J Clin Nutr* 86: 899–906.
- Katakam PV, Ujhelyi MR, Hoenig ME, Miller AW (1998). Endothelial dysfunction precedes hypertension in diet-induced insulin resistance. *Am J Physiol* 275 (3 Pt 2): R788–R792.
- Kendall DM, Harmel AP (2002). The metabolic syndrome, type 2 diabetes, and cardiovascular disease: understanding the role of insulin resistance. *Am J Manag Care* 8 (Suppl. 20): S635–S653. Quiz S654–S637.
- Kim JA, Montagnani M, Koh KK, Quon MJ (2006). Reciprocal relationships between insulin resistance and endothelial dysfunction: molecular and pathophysiological mechanisms. *Circulation* 113: 1888–1904.
- Kotchen TA, Reddy S, Zhang HY (1997). Increasing insulin sensitivity lowers blood pressure in the fructose-fed rat. *Am J Hypertens* 10 (9 Pt 1): 1020–1026.
- Kwan JA, Schulze CJ, Wang W, Leon H, Sariahmetoglu M, Sung M *et al.* (2004). Matrix metalloproteinase-2 (MMP-2) is present in the nucleus of cardiac myocytes and is capable of cleaving poly (ADP-ribose) polymerase (PARP) in vitro. *FASEB J* 18: 690–692.
- Lee MK, Miles PD, Khouresheed M, Gao KM, Moossa AR, Olefsky JM (1994). Metabolic effects of troglitazone on fructose-induced insulin resistance in the rat. *Diabetes* 43: 1435–1439.
- Matsuda M, DeFronzo RA (1999). Insulin sensitivity indices obtained from oral glucose tolerance testing: comparison with the euglycemic insulin clamp. *Diabetes Care* 22: 1462–1470.
- Murphy G, Willenbrock F, Crabbe T, O'Shea M, Ward R, Atkinson S *et al.* (1994). Regulation of matrix metalloproteinase activity. *Ann N Y Acad Sci* 732: 31–41.
- Nagareddy PR, MacLeod KM, McNeill JH (2010). GPCR agonist-induced transactivation of the EGFR upregulates MLC II expression and promotes hypertension in insulin-resistant rats. *Cardiovasc Res* 87: 177–186.

Panza JA, Casino PR, Kilcoyne CM, Quyyumi AA (1994). Impaired endothelium-dependent vasodilation in patients with essential hypertension: evidence that the abnormality is not at the muscarinic receptor level. *J Am Coll Cardiol* 23: 1610–1616.

Puyraimond A, Fridman R, Lemesle M, Arbeille B, Menashi S (2001). MMP-2 colocalizes with caveolae on the surface of endothelial cells. *Exp Cell Res* 262: 28–36.

Reaven GM (1991). Abnormalities of carbohydrate and lipoprotein metabolism in patients with hypertension. Relationship to obesity. *Ann Epidemiol* 1: 305–311.

Rodrigues SF, Tran ED, Fortes ZB, Schmid-Schonbein GW (2010). Matrix metalloproteinases cleave the beta2-adrenergic receptor in spontaneously hypertensive rats. *Am J Physiol Heart Circ Physiol* 299: H25–H35.

Sawicki G, Leon H, Sawicka J, Sariahmetoglu M, Schulze CJ, Scott PG *et al.* (2005). Degradation of myosin light chain in isolated rat hearts subjected to ischemia-reperfusion injury: a new intracellular target for matrix metalloproteinase-2. *Circulation* 112: 544–552.

Smith GN Jr, Brandt KD, Hasty KA (1996). Activation of recombinant human neutrophil procollagenase in the presence of doxycycline results in fragmentation of the enzyme and loss of enzyme activity. *Arthritis Rheum* 39: 235–244.

Song D, Hutchings S, Pang CC (2005). Chronic N-acetylcysteine prevents fructose-induced insulin resistance and hypertension in rats. *Eur J Pharmacol* 508: 205–210.

Tran LT, Yuen VG, McNeill JH (2009). The fructose-fed rat: a review on the mechanisms of fructose-induced insulin resistance and hypertension. *Mol Cell Biochem* 332: 145–159.

Tran ED, DeLano FA, Schmid-Schonbein GW (2010). Enhanced matrix metalloproteinase activity in the spontaneously hypertensive rat: VEGFR-2 cleavage, endothelial apoptosis, and capillary rarefaction. *J Vasc Res* 47: 423–431.

Vasudevan H, Nagareddy PR, McNeill JH (2006). Gonadectomy prevents endothelial dysfunction in fructose-fed male rats, a factor contributing to the development of hypertension. *Am J Physiol Heart Circ Physiol* 291: H3058–H3064.

Verma S, Bhanot S, McNeill JH (1994). Antihypertensive effects of metformin in fructose-fed hyperinsulinemic, hypertensive rats. *J Pharmacol Exp Ther* 271: 1334–1337.

Verma S, Bhanot S, McNeill JH (1995). Effect of chronic endothelin blockade in hyperinsulinemic hypertensive rats. *Am J Physiol* 269: H2017–H2021.

Verma S, Bhanot S, Yao L, McNeill JH (1996). Defective endothelium-dependent relaxation in fructose-hypertensive rats. *Am J Hypertens* 9 (4 Pt 1): 370–376.

Verma S, Bhanot S, McNeill JH (1999). Sympathectomy prevents fructose-induced hyperinsulinemia and hypertension. *Eur J Pharmacol* 373: R1–R4.

Wang W, Schulze CJ, Suarez-Pinzon WL, Dyck JR, Sawicki G, Schulz R (2002). Intracellular action of matrix metalloproteinase-2 accounts for acute myocardial ischemia and reperfusion injury. *Circulation* 106: 1543–1549.

Yao JS, Shen F, Young WL, Yang GY (2007). Comparison of doxycycline and minocycline in the inhibition of VEGF-induced smooth muscle cell migration. *Neurochem Int* 50: 524–530.

Zavaroni I, Mazza S, Dall'Aglia E, Gasparini P, Passeri M, Reaven GM (1992). Prevalence of hyperinsulinaemia in patients with high blood pressure. *J Intern Med* 231: 235–240.

Supporting information

Additional Supporting Information may be found in the online version of this article:

Figure S1 Effect of doxycycline on insulin resistance. (A) Phospho and total IRS1 expression in SMAs from control and FHRs. Representative Western blot showing phospho (tyr989) and total IRS1 expression, with GAPDH as a loading control. The densitometric values of phospho-IRS1 were normalized to their corresponding total IRS densitometric values and the relative band intensities are expressed as mean \pm SEM ($n = 8$). *Different from all groups ($P < 0.05$). Open bars represent control groups and solid bars represent fructose-fed rats. (B) Phospho and total Akt expression in SMAs of control and FHRs. Representative Western blot showing phospho (Akt473) and total Akt expression, with GAPDH as a loading control. The densitometric values of phospho-Akt were normalized to their corresponding total Akt densitometric values and the relative band intensities are expressed as mean \pm SEM ($n = 8$). *Different from all groups ($P < 0.05$). Open bars represent control groups and solid bars represent fructose-fed rats.

Figure S2 Representative photomicrographs illustrating the extent of co-localization (overlap) of MMP-2 and HSP90 in BCAE cells. BCAE cells were grown on poly-D-lysine coated cover slips in a 24-well plates. Control and Con A treated cells were fixed with 4% paraformaldehyde. Cells were treated with MMP-2 and HSP-90 primary antibodies for 24 h and incubated with goat anti-mouse Alexa 488 (green) and goat anti-rabbit Alexa 594 (red). Panels A and D represent images taken in red 8-bit channel and B and E in green 8-bit channel. Panels C and F images are generated from ImageJ and the co-localization highlighter plug-in showing the extent of overlap (co-localization) in white colour.

Figure S3 Representative photomicrographs illustrating the extent of co-localization (overlap) of MMP-2 and eNOS in BCAE cells. Representative photomicrographs showing co-localization of eNOS and MMP-2 in control and Con A treated BCAE cells. Panels A–C represent control cell images taken in red and green 8-bit channels and merged using ImageJ software. The extent of co-localization is shown in white colour generated via co-localization highlighter plug-in; panels D–F represent cells showing increased co-localization in cells after Con A treatment.

Please note: Wiley-Blackwell are not responsible for the content or functionality of any supporting materials supplied by the authors. Any queries (other than missing material) should be directed to the corresponding author for the article.